Bioinorganic Chemistry

The Geometric and Electronic Structure of [(cyclam-acetato)Fe(N)]$^+$: A Genuine Iron(V) Species with a Ground-State Spin $S = 1/2$**

Núria Aliaga-Alcalde, Serena DeBeer George, Bernd Mienert, Eckhard Bill, Karl Wieghardt, and Frank Neese**

High-valent transition-metal complexes play a crucial role as intermediates in the reaction cycles of metalloenzymes[1,2] and, consequently, the synthesis of low-molecular-weight compounds that model the active sites is a major challenge in synthetic inorganic chemistry. Many of these observed heme- and non-heme enzyme intermediates contain terminal oxo ligands.[2] While in recent years a number of heme- and non-heme Fe^{IV}=O complexes have been prepared and spectroscopically characterized,[3] much less is known about the corresponding high-valent iron–nitrido species despite their possible involvement in enzymes from the biogeochemical nitrogen cycle. However, over the course of the last few years a number of high-valent non-heme metal–nitrido species containing V^V, Cr^V, Mn^V, and Fe^V ions have been prepared by atom and/or group-transfer reactions or by photolysis.[4,5] We note that Wagner and Nakamoto[5c,d] have previously reported the photochemical generation of $[Fe^V(N)(TPP)$ (TPP^{2-} = tetraphenylporphinate(2−)) and measured its resonance Raman spectrum. Most recently, Betley and Peters synthesized and characterized the distorted tetrahedrally coordinated terminal Fe^{IV}–nitrido species $[PhBP^iPr_3]Fe^{IV}N$ ($[PhBP^iPr_3] = [PhB(CH_2P^iPr_2)_3]^-$).[6] This compound was shown to be diamagnetic at room temperature and exhibit ^{15}N NMR resonances near $\delta = 952$ ppm and a ν(FeN) stretching frequency of 1034 cm^{-1}. Furthermore, density functional theory (DFT) calculations at the B3LYP level of theory predicted a very short Fe≡N bond of 1.49 Å.

Efforts in our group to characterize high-valent iron–nitrido species started with the synthesis of two non-heme azidoiron(III) precursors, *cis*- (**1**) and *trans*-$[(cyclam)Fe^{III}(N_3)_2](ClO_4)$ (**2**), by using the spectroscopically innocent ligand cyclam (1,4,8,11-tetrazacyclotetradecane).[5a] Photolysis of **2** in a frozen matrix yielded products that were assigned to Fe^{II} (ca. 29%) and Fe^V (ca. 54%) species on the basis of zero-field Mössbauer spectroscopy.[5a] It was concluded that homolytic Fe–N_3 cleavage (to give Fe^{II} and $N_3^{\bullet}$; photoreduction) and heterolytic N–N cleavage (to give Fe^VN and N_2; photooxidation) both occur.[5a] Subsequently, the synthesis and photolysis of $[(cyclam\text{-}ac)Fe(N_3)]^+$ (cyclam-ac^- = 1,4,8,11-tetraazacyclotetradecane-1-acetate) (**3**) was reported.[5b] It was shown that photolysis at $\lambda > 420$ nm, that is, irradiation into the $N_3^- \rightarrow Fe$ ligand-to-metal charge transfer band at 80 K, resulted in >80% conversion to the desired $[(cyclam\text{-}ac)Fe(N)]^+$ species (**3ox**) and dinitrogen. A spin state of $S = 3/2$ was initially proposed for complex **3ox** by comparing the field-dependent Mössbauer spectra (>1 T) with previous data for complex **2**.[5b]

We have now undertaken an in depth spectroscopic and computational study of **3** and **3ox** to elucidate the electronic structure of this fascinating high-valent system. Herein, we present our initial results of X-ray absorption spectroscopy (XAS)/extended X-ray absorption fine structure (EXAFS) spectroscopy together with Mössbauer spectroscopy, magnetic susceptibility data, and electronic structure calculations at the density functional theory (DFT) level. The results reveal that, unexpectedly, the ground-state total spin of the $(FeN)^{2+}$ core is $S = 1/2$ and not $S = 3/2$ as has been previously assumed based on the results of EPR and Mössbauer spectroscopy.[5]

The fitting of the zero-field Mössbauer spectra[5b] of a solid sample of **3**, which was irradiated at 80 K, shows the superposition of two subspectra (not shown): a minor quadrupole doublet (ca. 16% relative intensity) with parameters corresponding to the starting material (**3**), with a chemical shift $\delta = 0.27(2)$ mm s^{-1} and a quadrupole splitting of $|\Delta E_q| = 2.30(2)$ mm s^{-1}, and second, an intense symmetric quadrupole doublet at $\delta = -0.02(2)$ mm s^{-1} with a quadrupole splitting of $|\Delta E_q| = 1.60(2)$ mm s^{-1} (**3ox**, ca. 84% relative intensity). Other side products were not observed in the solid sample of **3ox**. The values of the isomer shift and quadrupole splitting of the main solid beige species were very similar to those found in the past for $[(cyclam\text{-}ac)Fe(N)]^+$ in acetonitrile solution ($\delta = -0.04(2)$ mm s^{-1} and $|\Delta E_q| = 1.67(2)$ mm s^{-1}).[5b] It is therefore concluded that photolysis in the solid state is an efficient method to obtain high yields of solid **3ox** without the presence of the photoreduced Fe^{II} species. Moreover, the photooxidized species produced by photolysis in frozen solution and in the solid state are spectroscopically indistinguishable.

The Mössbauer results, in particular, the low isomer shift of **3ox**, are consistent with a high-valent species and have previously led to the formulation of **3ox** as an Fe^V species.[5] Independent experimental data to corroborate this conclusion and to obtain further information about the electronic and geometric structure of **3ox** are highly desirable. An ideal local probe of the geometric and electronic structure of the central iron is XAS. The XAS edge is sensitive to the electronic structure and may be used as an indicator of the oxidation state.[7,8] The pre-edge region is particularly diag-

[*] Dr. N. Aliaga-Alcalde, B. Mienert, Dr. E. Bill, Prof. Dr. K. Wieghardt, Priv.-Doz. Dr. F. Neese
Max Planck Institut für Bioanorganische Chemie
Stiftstrasse 34–36, 45470 Mülheim an der Ruhr (Germany)
Fax: (+49) 208-306-3951
E-mail: wieghardt@mpi-muelheim.mpg.de
neese@mpi-muelheim.mpg.de
Dr. S. DeBeer George
Stanford Synchrotron Radiation Laboratory
SLAC, Stanford University, Stanford, CA 94309 (USA)

[**] N.A.A. thanks the Max Planck society for a postdoctoral fellowship. SSRL operations are funded by DOE, BES. The SMB program is supported by NIH, NCRR, BMTP and by DOE, BER. S.D.G. thanks Prof. J. I. Brauman and Dr. D. Walthall for use of their xenon arc lamp. Cyclam-acetato = 1,4,8,11-tetraazacyclotetradecane-1-acetato.

Supporting information for this article is available on the WWW under http://www.angewandte.org or from the author.

  DOI: 10.1002/ange.200462368

nostic and an increase of about 1 eV per oxidation state is typical for first-row transition metals. In addition, the pre-edge region provides a measure of 3d–4p mixing and thus increased intensity may be induced by exceptionally short metal–ligand bonds. EXAFS data give complimentary metrical information, providing very accurate metal–ligand bond lengths.

A comparison of the Fe K-edge spectra of **3** and **3ox**, which, for technical reasons, were recorded in frozen butyronitrile solution, is shown in Figure 1. It is observed that the

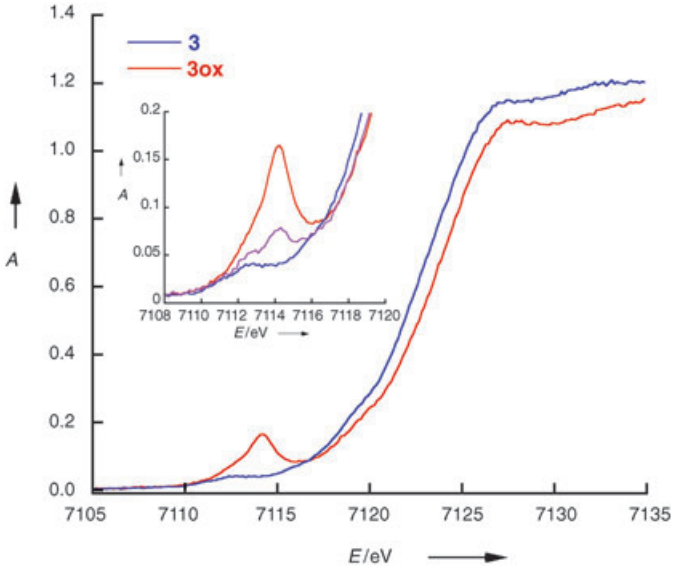

Figure 1. Iron K-edge X-ray absorption spectra of **3** (blue) and **3ox** (red). The inset is an expansion of the pre-edge region. The spectrum shown in purple was taken at an intermediate stage of illumination. *A* = normalized absorption.

pre-edge of **3ox** (at 7114.2 eV) is shifted to higher energy than **3** by about 2 eV (Fe^{III}; 7112.4 eV), consistent with a two-electron oxidation. To our knowledge, the pre-edge position of **3ox** is at the highest yet observed energy for any iron complex ($Fe^{IV}O$ edges are typically observed at about 7113.2 eV,[9] when using a reference calibration point of 7111.2 eV for the first inflection point of an Fe foil). The position of the rising edge (7123.0 eV for **3** versus 7124.1 eV for **3ox**) is also consistent with an increase in oxidation state; however, an exact assignment may be complicated by the presence of shake-up or shake-down transitions superimposed on the rising edge. Furthermore, a very intense pre-edge feature develops in **3ox** (with an area of 27 ± 2 units) at about 7114.2 eV, which is consistent with grossly increased 4p mixing into the 3d manifold and consequently with a short metal–ligand bond being formed in **3ox**. Similar features have previously been observed in high-valent $Fe^{IV}O$ species[9] and appear to be characteristic of high-valent sites with a short metal–ligand bond.

Figure 2 shows a comparison of the non-phase shift corrected Fourier transforms and EXAFS data, together with the best fits (Table 1), for complexes **3** and **3ox**. The best fit of complex **3** was obtained by including two Fe–N/O

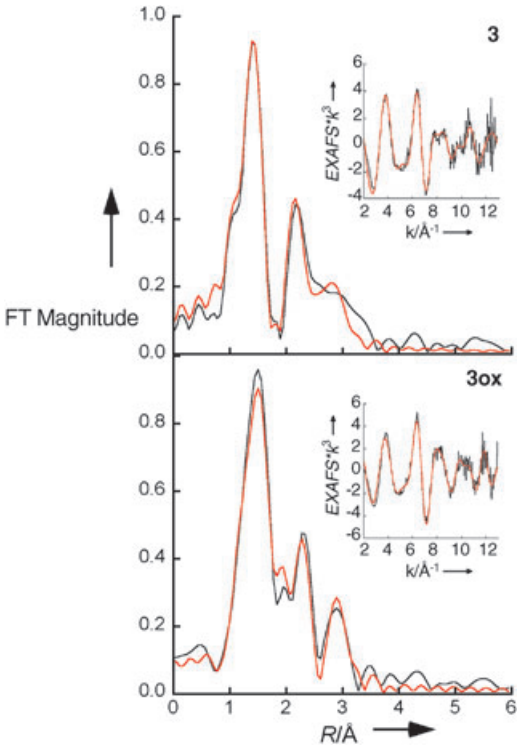

Figure 2. Comparison of non-phase shift corrected Fourier transforms for **3** and **3ox**. Experimental data are shown in black and fits in red. The insets show the respective EXAFS data.

Table 1: EXAFS fit results for **3** and **3ox**.

	R [Å]	σ^2 [Å^2]	ΔE_0	Error[a]
		3		
2 Fe–N/O	1.94	0.0018	−9.25	0.353
4 Fe–N/O	2.07	0.0064		
6 Fe–C	2.83	0.0063		
4 Fe–C	3.00	0.0032		
2 Fe–C	3.39	0.0026		
		3ox		
1 Fe–N	1.61	0.0144	−8.59	0.292
5 Fe–N/O	2.02	0.0079		
6 Fe–C	2.85	0.0047		
4 Fe–C	3.02	0.0033		
2 Fe–C	3.36	0.0026		

[a] Error is given by $\Sigma[(\chi_{obsd}-\chi_{calcd})^2 k^6]/\Sigma[(\chi_{obsd}{}^2 k^6]$.

contributions at a distance of 1.94 Å and four Fe–N/O at 2.07 Å, with outer-shell Fe–C contributions from the cyclam ligand (Figure 2, top). It should be noted that separation of these two contributions is just beyond the resolution limit of the data (ca. 0.14 Å). Fits were also attempted with a single Fe–N/O shell at 1.98 Å, giving excellent agreement with the crystallographic values,[5b] but a significantly larger residual. In either case an average Fe–N/O coordination sphere of 1.98–2.03 Å is obtained, in reasonable agreement with the crystallography.

The best fit to **3ox** (Figure 2, bottom) was obtained by including five Fe–N/O contributions at 2.02 Å and one short Fe–N distance at 1.61 Å, with additional outershell Fe–C contributions from the cyclam ligand. However, the Debye–

Waller value (σ^2) for the short Fe–N component is quite large. This value becomes much more reasonable[10] (0.006 Å^2) by decreasing the coordination number associated with the short Fe=N interaction to 0.5. The necessity of this decrease is consistent with incomplete conversion of **3ox**, as discussed above. Fits which did not include the short 1.61 Å Fe–N interaction had a significantly higher error (normalized error = 0.403) and a long frequency beat pattern, consistent with a short Fe–N vector, in the fit residual (see Supporting Information) which is clearly not observed for in the residual of **3** (see Supporting Information).[11] In addition, fits were also attempted starting with the short Fe–N distance at 1.73 Å, however, allowing this value to float resulted in a value of 1.60 Å for the shortest Fe–N distance. Finally, any attempt to modify the background subtraction always led back to the conclusion that the longest feasible Fe=N distance is $\leq$1.65 Å. We conclude from this data that there indeed is a short Fe=N bond of about 1.60 Å in **3ox**.

In our DFT calculations, we have considered two possible reaction products that differ in their spin multiplicities: a doublet (^{2}**3ox**) and a quartet (^{4}**3ox**) ground state were taken into consideration. Previously, the reaction was assumed to lead to a quartet species ^{4}**3ox** despite this being a spin-forbidden process. At the time this appeared to be reasonable because Fe^{V} species (d^3) are isoelectronic with the analogous Cr^{III} and Mn^{IV} species which invariably have $S = 3/2$ ground states. Quite surprisingly, the B3LYP DFT calculations on **3ox** even after inclusion of zero-point energies and solvent effects predict a doublet ground state ^{2}**3ox** (Figure 3).

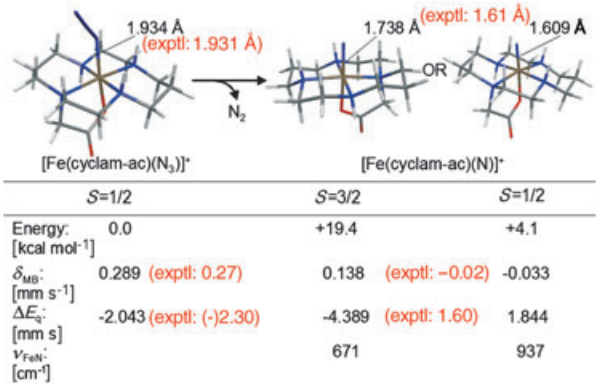

Figure 3. Computed structures, energies, and properties of **3ox**, ^{4}**3ox**, and ^{2}**3ox** (experimental values in red).

However, it is known that DFT methods are biased in favor of low-spin states.[12] Thus, despite the considerable energy difference of about 15 kcal mol^{-1} (ca. 14 kcal mol^{-1} in MeCN) between ^{2}**3ox** and ^{4}**3ox**, which is outside the accepted error bars of the B3LYP method, one is well advised in seeking more evidence in favor of such an unusual spin-state assignment. As will be elaborated in detail elsewhere, the magnetic properties of **3ox** are not straightforwardly interpreted, owing to the presence of other doublet and quartet terms lying close to the ground state. Thus, EPR, MCD, and magnetic Mössbauer analyses require a more elaborate spin Hamiltonian model than is usual for $S = 1/2$. However, the presence of a doublet ^{2}**3ox** species could be experimentally corroborated from a magnetic susceptibility measurement (Figure 4). Since the macroscopic susceptibility data are much less sensitive to details of the electronic structure, we could

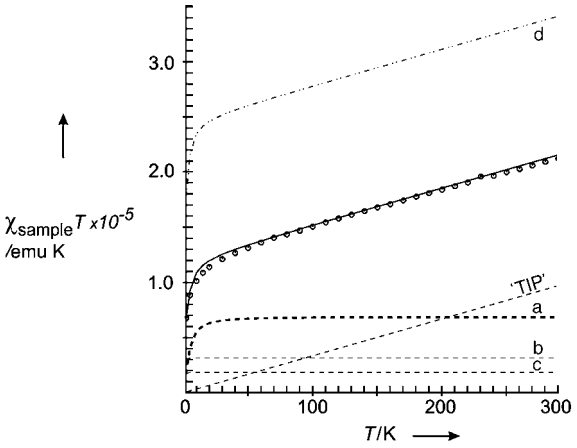

Figure 4. Temperature dependence of the magnetic susceptibility times temperature of a powder sample of photolyzed **3** (open circles) and deconvolution into three major paramagnetic components (traces a–c) and a TIP-like contribution ('TIP', temperature-independent paramagnetism). The 'TIP' arises most probably from minor contamination of small magnetic (oxide) particles (2%). The weights of the different paramagnetic contributions are given in molar percentages that were calculated with molecular weights of $M_r = 472.1$ g mol^{-1} (**3ox**, $S = 1/2$, 57%, trace a), $M_r = 500.1$ g mol^{-1} (**3**, 26%, $S = 1/2$, trace b), $M_r = 458.1$ g mol^{-1} ([(cyclam-ac)Fe^{II})], $S = 2$, 15%, trace c). Diamagnetic contributions were not taken into account since their signal is hidden under the 'TIP' contribution. The dashed lines for the contributions from ^{2}**3ox**, **3**, and the Fe^{II} component are simulations with the usual spin-Hamiltonian.[5a] The upper line in the graph (d) corresponds to the fitting of the data when the spin ground state of **3ox** is taken to be $S = 3/2$.

apply the usual spin Hamiltonian approach for a simulation of the temperature-dependence of χT for a powder sample. The data are perfectly deconvoluted into three paramagnetic contributions, namely from the remaining starting complex **3** (26%, $S = 1/2$) and an Fe^{II} contamination from some photoreduction (15%, $S = 2$), and from the target material ^{2}**3ox** which is the major component (57%, $S = 1/2$). Since the relative amounts of the different constituents correspond within a narrow error margin of $\pm$1.4% of an 80 K Mössbauer spectrum of an aliquot of the SQUID sample (see Supporting Information), we trust that **3ox** in fact has indeed the postulated doublet ground state. By contrast, the trace (d) in Figure 4 demonstrates that there it is not possible to fit the data under the assumption of a $S = 3/2$ ground state for **3ox**.

Rather interestingly, the optimized structures of ^{2}**3ox** and ^{4}**3ox** show a large difference in the computed Fe=N bond lengths, which are 1.609 Å for ^{2}**3ox** and 1.738 Å for ^{4}**3ox**. We note that the Fe^{III}–N_3 distance in low-spin **3** is accurately predicted by the calculations (1.934 Å calculated versus 1.931 Å (X-ray) and 1.94 Å (EXAFS)). Since DFT is typically accurate within 0.01–0.03 Å for short and strong metal–ligand bonds such as the ones formed with oxo ligands in complexes

analogous to **3** and **3ox**,[5b,10] this provides strong evidence that the short Fe=N bond observed by EXAFS spectroscopy indeed corresponds to ^{2}**3ox** and not to ^{4}**3ox**.

Further strong evidence for the doublet ground state of **3ox** is obtained from the calculated Mössbauer parameters of ^{2}**3ox** and ^{4}**3ox**: the calculated isomer shifts are -0.033 mm s^{-1} and 0.138 mm s^{-1}, respectively. Thus, the experimental value of -0.02 mm s^{-1} agrees only with the computed isomer shift of ^{2}**3ox**. Based on previous isomer shift calculations, the error in the predicted value is expected to be less than 0.1 mm s^{-1}.[10,13,14] Consequently, the calculations provide strong evidence for ^{2}**3ox** and not ^{4}**3ox** being the observed species. The calculation of the quadrupole splitting is in line with this result, giving values of -4.39 mm s^{-1} for ^{4}**3ox** and $+1.84$ mm s^{-1} for ^{2}**3ox** compared with the experimental value of $|\Delta E_q| = 1.60$ mm s^{-1}. The large value calculated for ^{4}**3ox** is far from that derived from the experiment and outside the error bar of the calculations which usually give results within about 0.3 mm s^{-1} of those from the experiment even in complicated bonding situations.[14,10] As an independent check we note that the Mössbauer parameters calculated for **3** are in excellent agreement with the experimental values ($\delta_{calcd} = 0.289$ mm s^{-1}, $\delta_{exptl} = 0.27$ mm s^{-1}; $|\Delta E_q^{calcd}| = 2.04$ mm s^{-1}, $|\Delta E_q^{exptl}| = 2.30$ mm s^{-1}).

Having fairly rigorously established that ^{2}**3ox** is the species produced in the photolysis experiments, we want to briefly comment on the nature of the iron–nitrido bond in this unprecedented bonding situation (Figure 5). It is well known

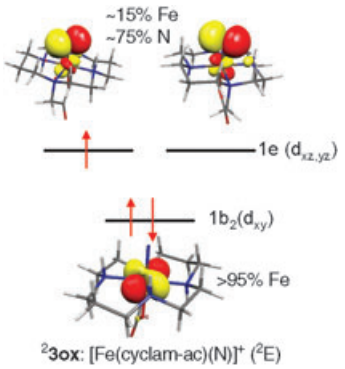

Figure 5. Ground-state electronic configuration of ^{2}**3ox**. The quartet state configuration is obtained by occupying all three MOs with one spin-up electron.

that in distorted octahedral environments the metal d orbitals split into an (almost) degenerate π-(anti)bonding t_{2g} and an (almost) degenerate σ-(anti)bonding set. However, if there is a dominant short metal–ligand bond, as in the present case of high-valent species, the splittings in both sets may become very large and often exceed 1 eV.[4h] In this case, the general rules about relative spin-state energetics as contained in the Tanabe–Sugano diagrams for octahedral symmetry may fail to hold, and in addition, there will be a very large anisotropic covalency induced by the strongly covalent metal–ligand bonds to the terminal oxo or nitride ligand. For the d^3 system examined here, the splitting between the almost pure metal d_{xy} orbital and the metal-derived $d_{xz,yz}$ orbitals apparently becomes so large that it is energetically more favorable to assume the (orbitally degenerate) configuration $^{2}E((d_{xy})^2$-$(d_{xz,yz})^1)$ (in approximate C_{4v} symmetry) as compared to the "canonical" configuration $^{4}A_2((d_{xy})^1(d_{xz})^1(d_{yz})^1)$. This will be further elaborated by high-level multireference ab initio calculations together with the results from MCD spectroscopy in a forthcoming paper. We indeed observe in the DFT calculations a very large anisotropic covalency of the iron–nitrido bond with the two metal-derived $d_{xz,yz}$ orbitals having only about 15% metal and as much as 75% N character according to a Löwdin population analysis. Moreover, the 4p character in the unoccupied metal-d derived MOs increases from 0.2% in **3** to 5.8% in ^{4}**3ox** and 7.3% in ^{2}**3ox.** The dramatic increase in 4p character explains the very intense XAS pre-edge feature of **3ox** (despite the decrease in 3d character). The very low metal character in the formally metal $d_{xz,yz}$ orbitals is, to a certain extent, underestimated by DFT calculations. Highly correlated ab initio methods provide somewhat larger values. However, a very large amount of charge transfer from N^{3-} to Fe^{V} is already expected on electrostatic grounds. Thus, a possible formulation of the electronic structure as a resonance between $Fe^{V}(S_{Fe}=3/2)N^{3-}(S_N=0) \leftrightarrow Fe^{III}(S_{Fe}=1/2)N^{-}(S_N=1)$ seems plausible for ^{4}**3ox**, whereas ^{2}**3ox** may best be represented by the resonance structures of the type $Fe^{V}(S_{Fe}=1/2)N^{3-} \leftrightarrow Fe^{II}(S_{Fe}=0)N^{\cdot}(S_N=1/2)$. The system will nevertheless behave to a certain extent like a d^3 system and we prefer to formulate the species as an Fe^{V} species. It is noted that the amount of charge transfer from N^{3-} to Fe^{V} is much larger than from O^{2-} to Fe^{IV} in $(FeO)^{2+}$ where the metal-derived $d_{xz,yz}$ orbitals are more equally shared between Fe and O.[3b,15]

The large calculated increase in Fe–N distance of about 0.13 Å in ^{4}**3ox** compared to ^{2}**3ox** is nicely explained by the strongly antibonding character of the $1e(d_{xz,yz})$ set, which is doubly occupied in ^{4}**3ox** but only singly occupied in ^{2}**3ox**. Likewise, we have calculated an increase in the harmonic vibrational Fe=N stretching frequency from 671 cm^{-1} in ^{4}**3ox** to 937 cm^{-1} in ^{2}**3ox** corresponding to an increase in force constant from about 0.19 mdyn Å^{-1} to about 0.42 mdyn Å^{-1}. These numbers tend to be reliable from DFT but an independent experimental confirmation is, unfortunately, missing. In terms of formal bond order, one has to view the $(FeN)^{2+}$ core as a highly covalent unit with a double bond in ^{4}**3ox** and a bond of order 2.5 in ^{2}**3ox**. It is most intriguing that the ground state of ^{2}**3ox** is (almost) orbitally degenerate and will thus feature two low-lying Kramers doublets. As will be elaborated in detail elsewhere, this situation is experimentally difficult to distinguish from a zero-field split spin quartet state and leads to fascinatingly complicated magnetic behavior.

In summary, we have shown in this work through a combination of theory and experiment that photolysis of the non-heme Fe^{III}–N_3^- complex **3** in the solid state nearly quantitatively affords the desired genuine Fe^{V}–nitrido complex **3ox**. This complex features a highly unusual, almost orbitally degenerate, spin doublet ground state with a short (1.60 Å) Fe=N distance corresponding to a Fe=N bond of order 2.5. While in terms of the formal oxidation state, there is no doubt that **3ox** is to be formulated as an iron(v) species, the spectroscopic oxidation state[16] in this system is much harder

to determine unambiguously. In particular, the XAS and Mössbauer parameters are in full agreement with a highly oxidized iron center, whereas the DFT calculations, which lead to agreement with the spectroscopic experiments, show an excessive transfer of negative charge from the nitride ligand to the central iron.

Experimental Section

The irradiation process of **3** was performed on a suspension of powder samples in liquid N_2 over 4 h with a Rayonet Photochemical Reactor (RPR-100) equipped with 419 nm tubes. The photolysis process was followed optically by changes in the color of the species, from red-brown to pale beige, and monitored by IR spectroscopy. Mössbauer and magnetic susceptibility data were collected and analyzed as reported previously.[5] For SQUID measurements (radiation for about 10 h), the sample powder was not in direct contact with liquid N_2, but sealed in a flask to avoid condensation of water and subsequent deterioration during sample transfer to the SQUID magnetometer at ambient temperature.

XAS data for complexes **3** and **3ox** were recorded at the Stanford Synchrotron Radiation Laboratory (SSRL) on focused beam line 9–3, as previously described.[17] Internal energy calibration was performed by assigning the first inflection point of the Fe foil spectrum to 7111.2 eV. XAS samples of **3** (ca. 2 mM) were dissolved in degassed PrCN, loaded into 2 mm Lucite XAS cells with polypropylene windows and then frozen immediately in liquid nitrogen prior to XAS measurements. The photooxidation of **3** to **3ox** was performed in liquid N_2 by exposure for about 1.5 h to a 1000 W Xenon arc lamp equipped with a monochromator and a long pass filter for energy selection at 420 nm. During XAS measurements, samples were maintained at a constant temperature of 10 K by an Oxford Instruments CF1208 continuous-flow liquid-helium cryostat. Data were processed and analyzed as described in reference [17]. Samples were monitored for photoreduction throughout the course of data collection. Only those scans, which showed no evidence of photoreduction were included in the final averages.

Electronic structure calculations were performed with the program package ORCA developed in our laboratory. Structures were optimized at the BP86 level of DFT with polarized triple-ζ basis sets.[18] Calculation of the harmonic force fields of all species at the same level proved all structures to be local minima on the potential energy surface and provided vibrational frequencies used to calculate zero-point energies and thermal corrections. Total electronic energies were calculated with the TZVPP basis set and the B3LYP functional. The same functional was used together with special basis sets for the prediction of Mössbauer parameters.[14] Environmental effects were modeled with the conductor like screening model (COSMO) as implemented in ORCA and using acetonitrile ($\varepsilon = 36.6$) as solvent.

Received: October 20, 2004
Published online: April 21, 2005

Please note: Minor changes have been made to this manuscript since its publication in *Angewandte Chemie* EarlyView. The Editor.

Keywords: electronic structure · EXAFS spectroscopy · iron · Mössbauer spectroscopy · nitrido ligands

[1] L. D. Slep, F. Neese, *Angew. Chem.* **2003**, *115*, 3048; *Angew. Chem. Int. Ed.* **2003**, *42*, 2942, and references therein.
[2] a) M. Costas, M. P. Mehn, M. P. Jensen, L. Que, Jr., *Chem. Rev.* **2004**, *104*, 939; b) D. L. Harris, *Curr. Opin. Chem. Biol.* **2001**, *5*, 724.
[3] a) J.-U. Rohde, J.-H. In, M. H. Lim, W. W. Brennessel, M. R. Bukowski, A. Stubna, E. Münck, W. Nam, L. Que, Jr., *Science* **2003**, *299*, 1037; b) A. Decker, J.-U. Rhode, L. Que, Jr., E. I. Solomon, *J. Am. Chem. Soc.* **2004**, *126*, 5378.
[4] a) T. Jüstel, J. Bendix, N. Metzler-Nolte, T. Weyhermüller, B. Nuber, K. Wieghardt, *Inorg. Chem.* **1998**, *37*, 35; b) J. Bendix, K. Meyer, T. Weyhermüller, E. Bill, N. Metzler-Nolte, K. Wieghardt, *Inorg. Chem.* **1998**, *37*, 1767; c) T. Jüstel, M. Müller, T. Weyhermüller, C. Kressl, E. Bill, P. Hildebrandt, M. Lengen, M. Grodzicki, A. X. Trautwein, B. Nuber, K. Wieghardt, *Chem. Eur. J.* **1999**, *5*, 793; d) K. Meyer, J. Bendix, N. Metzler-Nolte, T. Weyhermüller, K. Wieghardt, *J. Am. Chem. Soc.* **1998**, *120*, 7260; e) K. Meyer, J. Bendix, E. Bill, T. Weyhermüller, K. Wieghardt, *Inorg. Chem.* **1998**, *37*, 5180; f) J. Bendix, T. Weyhermüller, E. Bill, K. Wieghardt, *Angew. Chem.* **1999**, *111*, 2932; *Angew. Chem. Int. Ed.* **1999**, *38*, 2766; g) J. Bendix, R. J. Deeth, T. Weyhermüller, E. Bill, K. Wieghardt, *Inorg. Chem.* **2000**, *39*, 930; h) C. A. Grapperhaus, E. Bill, T. Weyhermüller, F. Neese, K. Wieghardt, *Inorg. Chem.* **2001**, *40*, 4191, and references therein; i) J. Bendix, *J. Am. Chem. Soc.* **2003**, *125*, 13348; j) T. Birk, J. Bendix, *Inorg. Chem.* **2003**, *42*, 7608; k) M. H. Huynh, T. J. Meyer, M. A. Hiskey, D. L. Jameson, *J. Am. Chem. Soc.* **2004**, *126*, 3608; l) W.-L. -Man, T.-M. Tang, T.-W. Wong, T.-C. Lau, S.-M. Peng, W.-T. Wong, *J. Am. Chem. Soc.* **2004**, *126*, 478.
[5] a) K. Meyer, E. Bill, T. Weyhermüller, K. Wieghardt, *J. Am. Chem. Soc.* **1999**, *121*, 4859; b) C. A. Grapperhaus, B. Mienert, E. Bill, T. Weyhermüller, K. Wieghardt, *Inorg. Chem.* **2000**, *39*, 5306; c) W.-D. Wagner, J. Nakamoto, *J. Am. Chem. Soc.* **1988**, *110*, 4044; d) W.-D. Wagner, J. Nakamoto, *J. Am. Chem. Soc.* **1989**, *111*, 1590.
[6] T. A. Betley, J. C. Peters, *J. Am. Chem. Soc.* **2004**, *126*, 6252.
[7] J. L. DuBois, P. Mukherjee, T. D. P. Stack, B. Hedman, E. I. Solomon, K. O. Hodgson, *J. Am. Chem. Soc.* **2000**, *122*, 5775.
[8] T. E. Westre, P. Kennepohl, J. G. DeWitt, B. Hedman, K. O. Hodgson, E. I. Solomon, *J. Am. Chem. Soc.* **1997**, *119*, 6297.
[9] a) M. H. Lim, J.-U. Rohde, A. Stubna, M. R. Bukowski, M. Costas, R. Y. N. Ho, E. Münck, W. Nam, L. Que, Jr., *Proc. Natl. Acad. Sci. USA* **2003**, *100*, 3665; b) J.-U. Rohde, S. Torelli, X. Shan, M. H. Li, J. Kaizer, K. Chen, W. Nam, L. Que, Jr., *J. Am. Chem. Soc.* **2004**, *126*, 16750.
[10] L. D. Slep, A. Mijovilovich, W. Meyer-Klaucke, T. Weyhermüller, E. Bill, E. Bothe, F. Neese, K. Wieghardt, *J. Am. Chem. Soc.* **2003**, *125*, 15554.
[11] It should be noted that EXAFS fits were also performed on the sample at an intermediate stage of illumination, shown in Figure 1. These data clearly required a short Fe–N distance (1.61 Å) in the fit (see Figure S4–S6 in the Supporting Information), supporting the fact that the change in electronic structure is coupled to the formation of a short Fe–N bond (1.6 Å).
[12] a) M. Reiher, *Inorg. Chem.* **2002**, *41*, 6928; b) A. Fouqueau, S. Mer, M. E. Casida, L. M. L. Daku, A. Hauser, T. Mieva, F. Neese, *J. Chem. Phys.* **2004**, *120*, 9473.
[13] R. Garcia Serres, C. A. Grapperhaus, E. Bothe, E. Bill, T. Weyhermüller, F. Neese, K. Wieghardt, *J. Am. Chem. Soc.* **2004**, *126*, 5138.
[14] F. Neese, *Inorg. Chim. Acta* **2002**, *337C*, 181.
[15] F. Neese, J. M. Zaleski, K. E. Loeb, E. I. Solomon, *J. Am. Chem. Soc.* **2000**, *122*, 11703.
[16] C. K. Jörgensen in *Oxidation Numbers and Oxidation States*, Springer, Heidelberg, **1969**.
[17] E. C. Wasinger, N. Mitić, B. Hedman, J. Caradonna, E. I. Solomon, K. O. Hodgson, *Biochemistry* **2002**, *41*, 6211.
[18] TZVP: A. Schäfer, C. Huber, R. Ahlrichs, *J. Chem. Phys.* **1994**, *100*, 5829.

